DOI: 10.1002/anie.201310349

Gradients

Electrochemically Generated Gradients

*Sven O. Krabbenborg and Jurriaan Huskens**

Keywords:
electrochemistry · gradients · materials science · reactivity

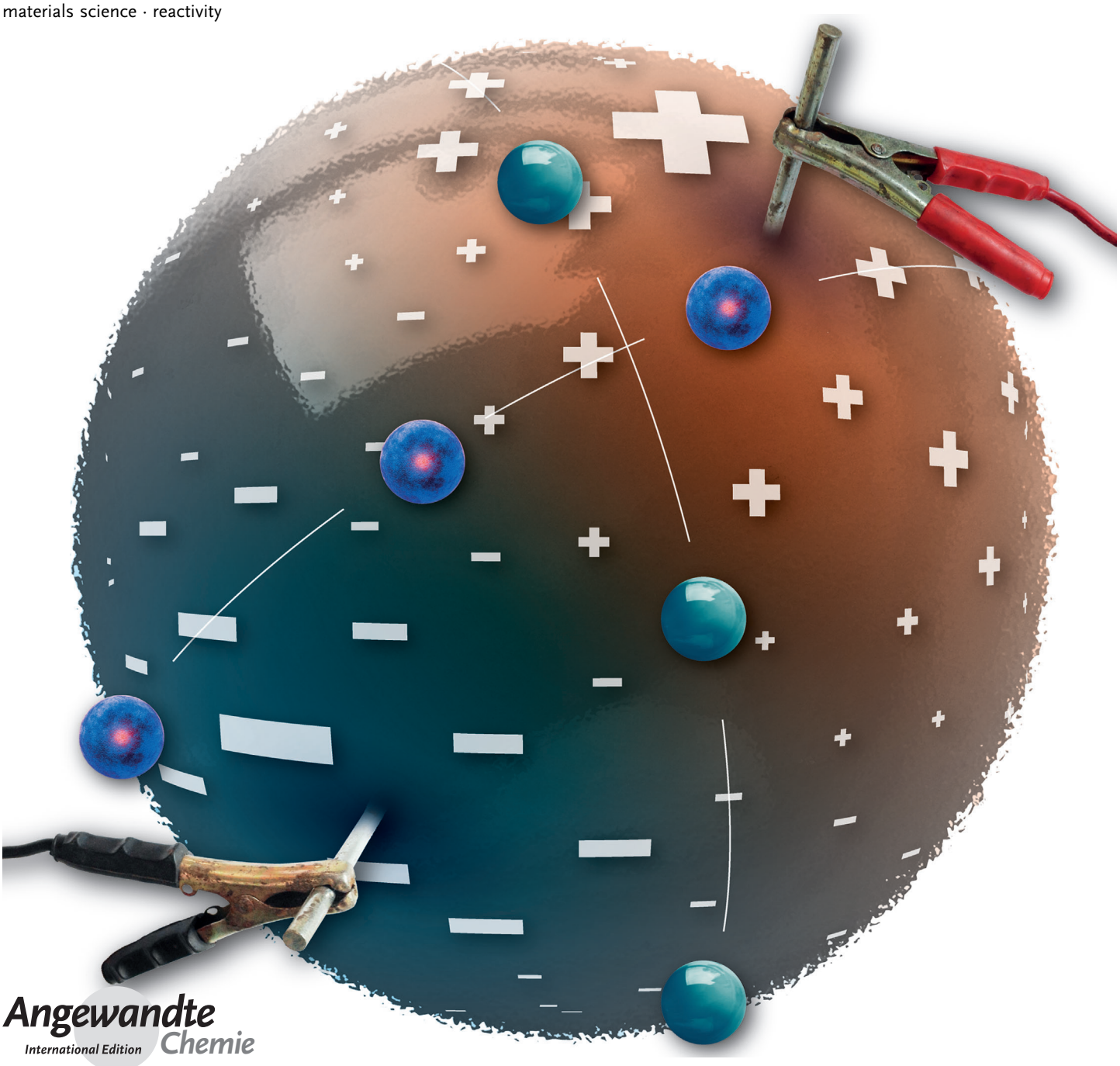

Angewandte International Edition Chemie

This review surveys recent developments in the field of electrochemically generated gradients. The gradual variation of properties, which is a key characteristic of gradients, is of eminent importance in technology, for example, directional wetting, as well as biology, for example, chemotaxis. Electrochemical techniques offer many benefits, such as the generation of dynamic solution and surface gradients, integration with electronics, and compatibility with automation. An overview is given of newly developed methods, from purely electrochemical techniques to the combination of electrochemistry with other methods. Electrochemically fabricated gradients are employed extensively for biological and technological applications, such as high-throughput screening, high-throughput deposition, and device development, all of which are covered herein. Especially promising are developments towards the study and control of dynamic phenomena, such as the directional motion of molecules, droplets, and cells.

From the Contents

1. Introduction

Gradients of physicochemical properties, that is, their continuous variation in space and/or time, are of great value both in solution and on surfaces for many applications and systems. These properties, such as the chemical composition in solution, the topography of a surface, and many others, can be tuned in length and shape, which is a key attribute of gradients.

Gradients play an important role in biological systems, both on surfaces (haptotaxis)[1] and in solution (chemotaxis),[2] and can occur both inter- and intracellularly.[2a,3] Biological gradients can be highly dynamic[4] and can display unexpected kinetic properties.[5] Such gradients have a spatiotemporal behavior that originates from autocatalysis, feedback, and other nonlinear influences.[6] When investigating such systems, it is therefore a necessity to mimic this dynamic behavior, and on the appropriate length scale. In the case of intercellular behavior, the length scale is on the order of 100 microns or below, whereas the size of the cell is the upper limit for intracellular systems.[1] Gradient-fabrication methods are gaining importance in biology for the study of cell behavior, such as the influence of extracellular gradients on chemotaxis and haptotaxis.[7] There have been several examples of the formation of artificial intracellular gradients: Gradients in enzyme were used to study their effect on the direction of cell motility,[8] whereas gradients in protein were applied to direct changes in cell morphology or polarize microtubule fibers.[9] Gradients are also utilized in the high-throughput screening of biomaterials.[10] The response of cells to roughness, which is of importance in the field of medical implants, was investigated by using samples containing a roughness gradient.[11]

Gradients are also employed in many technologically relevant applications, for example, in the high-throughput screening of materials,[12] such as catalysts[13] or sensing materials.[14] Composition gradients have been utilized for the discovery of new thin-film dielectrics.[15] Gradients are also employed when studying or driving motion, for example, the directional motion of water droplets by an interfacial-surface free-energy gradient[16] or by light-intensity gradients.[17] Gradients have even been utilized to steer molecular motion, such as the motion of dendrimer molecules on a gradient of aldehyde groups on a surface,[18] a single poly(ethylene glycol) molecule on an interfacial-surface free-energy gradient,[19] and multivalent ligand molecules along a receptor interface.[20]

Often applied gradient-fabrication techniques are based on diffusion, printing, dip coating, or irradiation.[21] For an overview of various chemical- and polymer-gradient-fabrication methods, the reader is referred to earlier reviews.[21,22] Almost all of the gradient-fabrication methods discussed therein produce gradients which are static, that is, once fabricated, the gradients have fixed physicochemical properties. For several applications, such as high-throughput screening, static gradients are appropriate. However, when aiming to control molecular/macroscopic motion or to study dynamic cell properties, it is a prerequisite that gradients can be switched on and off or the properties can be gradually changed over time. The ability to turn off the gradient is also convenient from an experimental point of view, as it provides a straightforward and reliable control without the driving force (the gradient).

Microfluidic gradient-fabrication techniques, for example, by means of laminar-flow mixing,[23] do offer the possibility to change solution-gradient properties in space and time and have been used for many biological applications.[24] Cell migration under the influence of solution gradients (chemotaxis),[7b,c] for example, has been studied extensively, even with a dynamic solution gradient.[25]

Whereas microfluidic gradient-fabrication techniques can create dynamic solution gradients, electrochemical gradient-fabrication techniques can also create dynamic surface

[*] Dr. S. O. Krabbenborg, Prof. Dr. J. Huskens
Molecular NanoFabrication Group
MESA+ Institute for Nanotechnology, University of Twente
P.O. Box 217, 7500 AE Enschede (The Netherlands)
E-mail: j.huskens@utwente.nl
Homepage: http://www.utwente.nl/tnw/mnf

gradients, which are essential for the study of haptotaxis and for dynamic cell-adhesion studies. The properties of gradients generated by electrochemical techniques can be influenced in several ways, such as by the positioning and arrangement of electrodes in combination with diffusion or by spatiotemporal variation of the applied potential. Electrochemical gradient-fabrication techniques have many additional beneficial properties. Electrochemical techniques are highly versatile, compatible with organic and inorganic systems and many solvents, and compatible with both conducting and nonconducting substrates. They can be integrated with electronics and are compatible with automation. There are also examples of gradients (based on so-called bipolar electrodes) that do not require leads, thus enabling more straightforward scaling up for high-throughput applications. In some configurations, electrochemistry can even be useful for quantitative analysis of the gradient.

There are many gradient-fabrication methods in which electrochemistry plays a role. The different methods are discussed in Section 2 of this Review. In Section 3, the diverse applications—first biological and then technological—of electrochemically fabricated gradients are described, with a particular focus on the fields of high-throughput screening/deposition, the driving of liquid motion, and cell-migration studies by the use of static and dynamic gradients, and the addition of functionality to devices.

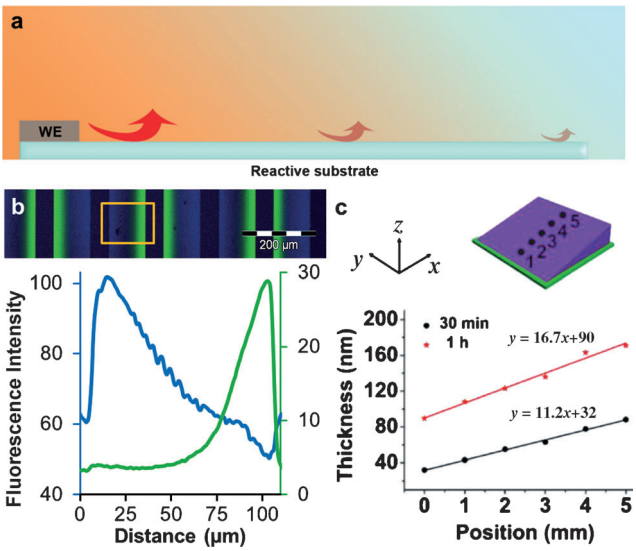

Figure 1. a) Creation of gradients by electrochemistry in combination with mass transfer. The species generated at the working electrode (WE) diffuses away, thus resulting in a concentration gradient of that species as a function of the distance to the electrode. This concentration gradient can be used to obtain a gradient in reactivity (red arrows). b) Fluorescence microscopy image (top) and corresponding fluorescence-intensity profiles (bottom) after the fabrication of bicomponent surface gradients of two different dyes.[29] Copyright 2013, The Royal Society of Chemistry. c) Thickness gradient of brushes prepared by SI-ATRP on Si, as a function of position and time.[30] Copyright 2013, American Chemical Society.

2. Electrochemical Gradient-Fabrication Methods

There are many different methods based on the use of electrochemistry to fabricate gradients. First, methods which rely solely on electrochemistry are discussed, followed by alternative methods which combine electrochemistry with the use of light, dip coating, or magnetic fields.

2.1. Electrochemical Gradients Created by Mass Transfer

One of the most straightforward methods for generating electrochemical gradients is based on mass transfer (Figure 1a). At the working electrode, an electrochemical reaction generates H_3O^+, OH^-, a catalyst, or any other species of interest, which diffuses away from the electrode, thus resulting in a concentration gradient of that species as a function of the distance to the electrode. This concentration gradient can be the desired result or, by the use of appropriate chemical reactions, can be used to obtain a gradient in reactivity, for example, at a substrate.

Abbott and co-workers described in 1999 the fabrication of electrochemically induced gradients in surface pressure.[26] This solution gradient originated from the generation of the surface-active species (11-ferrocenylundecyl)trimethylammonium at one electrode by reduction and its removal at the other electrode by oxidation.

Well-studied gradients fabricated electrochemically in combination with mass transfer are diffusion-based pH gradients, as commonly generated by the electrolysis of water on a small[27] or a larger scale.[28] These gradients typically belong to fully developed fields, such as isoelectric

Jurriaan Huskens obtained his PhD in 1994 with Herman van Bekkum from the Delft University of Technology. After postdoctoral studies with Dean Sherry and Manfred Reetz, he moved to the University of Twente in 1998, first as assistant professor with David Reinhoudt and since 2005 as full professor ("Molecular Nanofabrication"). His major research interests are supramolecular chemistry at interfaces and bottom-up nanofabrication. He received the Unilever Research Award 1990, a Marie Curie Fellowship (1997), and the Gold Medal 2007 of the Royal Netherlands Chemical Society.

Sven O. Krabbenborg obtained his MSc (2009, Cum Laude) in nanotechnology from the University of Twente with research supervised by Prof. Dr. Ir. Wilfred van der Wiel (University of Twente) and Prof. Jaume Veciana (Institute of Materials Science of Barcelona). He received his PhD (2014, Cum Laude) under the supervision of Prof. Dr. Ir. Jurriaan Huskens at the University of Twente. The aim of his project is the development and application of electrochemical methods for the generation of covalent and noncovalent surface gradients on the micron scale.

focusing and reversed-phase liquid chromatography, which fall outside the scope of this Review.

To circumvent problems that may occur during water electrolysis, for example, when high voltages or high current densities result in bubble formation or partial denaturation of proteins or enzymes, pH gradients have been formed by the electrochemical reduction of a "proton consumer". Yao and co-workers demonstrated such a process in 2007 by using *p*-benzoquinone or H_2O_2 as the proton consumer. The proton consumption that occurred during this electrochemical reaction gave rise to a pH gradient under much milder conditions than those used for the electrolysis of water.[31] An electrochemically active species was also used to prevent water electrolysis, in particular, to eliminate pH fluctuations, during the formation of noncovalent gradients of a charged dye-modified lipid and a protein by supported lipid bilayer electrophoresis.[32]

We recently employed platinum microelectrode arrays on glass for the establishment of a Cu^+ solution gradient by the local electrochemical reduction of Cu^{2+} at the cathode and oxidation of the generated Cu^+ back to Cu^{2+} at the anode under ambient conditions.[29,33] The Cu^+ generated was used for a copper(I)-catalyzed azide–alkyne 1,3-dipolar cycloaddition (CuAAC; "click" reaction), which enabled the attachment of functional molecules to azide-terminated surfaces. This method was used to fabricate 1D and 2D gradients of alkyne-modified dyes (Figure 1b) and alkyne-modified biotin on the micron scale, both in between the electrodes and on external substrates.

The method was also applied to polymer gradients by the use of surface-initiated atom-transfer radical polymerization (SI-ATRP) by Zhou and co-workers,[30] who fabricated gradients of grafted PSPMA brushes (Figure 1c) on conductive and nonconductive substrates (Si, PDMS, Ti, Au) covered with the corresponding initiator. A gradient in the concentration of the Cu^+ catalyst was obtained by tilting the substrates with respect to the working electrode.

A similar method was used by Oscarsson and co-workers to fabricate gradients on planar substrates and spherical particles.[34] Electrochemical oxidation of a gold electrode in a phosphate-buffered saline (PBS) solution led to the release of gold(III) chloride complexes, which reacted with thiols to form gold(I) thiolate complexes. The gold(I) thiolates in turn reacted with thiol-terminated molecules and proteins (in this case, immunoglobulin G labeled with fluorescein isothiocyanate, IgG(FITC)). Gradients on planar substrates were obtained by tilting the substrate with respect to the working electrode, thus yielding a gradient as a function of the distance to the working electrode. For spherical particles, nonconducting, thiolated magnetic beads were directed to the Au working electrode by a permanent magnet. A gradient in the gold(I) thiolate was formed by the distance dependence of the bead surface to the working electrode, and functionalization with IgG(FITC) in turn resulted in a gradient in protein on the bead surface.

A closely related method was used by Yousaf and co-workers.[35] The depletion of a hydroquinone-terminated thiol species in a microchannel, in combination with varying surface-exposure times, was used to generate a surface gradient of this thiol. The electrochemically active hydroquinone gradient was oxidized to the quinone form, which constituted a reactive gradient for the immobilization of an RGD–oxyamine peptide. This depletion method was used by the same group to form a gradient of I^- in combination with electrochemical Au etching.[36] The gold topography gradient formed in this way on glass was further functionalized with tetra(ethylene glycol)undecanethiol or -hexadecanethiol to give a cell-repelling or cell-spreading gradient, respectively.

2.2. Electrochemical Gradients Derived from In-Plane Potential Gradients

An often used and relatively simple method for fabricating gradients solely by electrochemistry involves the use of an in-plane potential gradient (Figure 2a). This method makes it possible to generate a gradient in electrochemical potential,

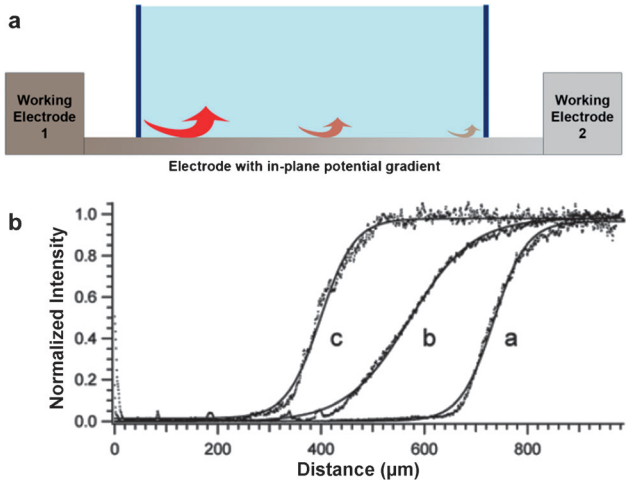

Figure 2. a) Creation of gradients by electrochemistry by the use of an in-plane potential gradient over a thin electrode. A reactivity gradient (red arrows) of an electrochemical reaction is formed. b) Normalized fluorescence profiles of gradients of fluorescently labeled NPs. The gradient center shifts according to the cathodic potential.[40] Copyright 2002, American Chemical Society.

which results in a gradient in reactivity, as a function of distance on the surface of a thin electrode. It relies on the relatively high resistance of the thin electrode (for example, Au with a thickness of < 50 nm). When different voltages are applied to the two working electrodes, the largest potential drop occurs over this thin electrode. If variations in roughness and thickness are disregarded, the potential gradient is linear.

In 2000, Bohn and co-workers described the use of this method to fabricate gradients on a gold electrode.[37] They created octanethiol gradients by the reductive desorption of thiols by using an in-plane potential gradient. The octanethiol-coverage gradient was backfilled with 3-mercaptopropanoic acid, thus resulting in a bicomponent gradient in surface free energy. By surface plasmon resonance (SPR), they showed that the application of gradually changing potentials enabled dynamic removal of the thiols, thus leading

to a shift in the boundary between thiol-covered and bare Au towards the anode.

This method was extended to the formation of other alkanethiol gradients exhibiting counterpropagating gradients in end-group or chain length.[38] Furthermore, it was shown that Cu gradients on Au could be deposited and stripped,[38a] down to a scale of tens of microns,[39] and that the oxidation of H_2O_2 could be controlled in a spatial manner to generate a gradient of O_2 bubble formation.[38a] In a similar way, gradients have been formed of fluorescently labeled nanoparticles (NPs),[40] of the extracellular matrix protein (ECM) fibronectin (FN),[41] of RGD peptides,[42] of signaling molecules, such as epidermal growth factor,[43] of polymers,[44] and of polymer brushes.[45] As an example, profiles of fluorescently labeled NP gradients fabricated by reductive desorption of 2-aminoethanethiol with an in-plane gradient are shown in Figure 2b. The profiles show clearly how the gradient centers shift according to the cathodic potential.

Hillier and co-workers used this method to deposit a surface-coverage gradient of a Pt catalyst on indium tin oxide (ITO) by inducing a gradient in the platinum-deposition rate.[46] They also used an in-plane potential gradient on an electrode surface consisting of a homogeneous Pt catalyst layer on ITO to produce pH gradients on the millimeter scale.[47] These pH gradients could be switched on and off, and both the position and magnitude of the change in the pH value could be controlled. Furthermore, the method of creating an in-plane potential gradient was expanded to the formation of 2D gradient patterns as shown for the electrodeposition of different polymers.[48]

Rubinstein and co-workers showed the formation of gradients in the height of electrodeposited nanowires (NWs) upon the deposition of Cu in nanoporous alumina membranes by using an in-plane potential gradient at the working electrode.[49] By using the same setup, they fabricated compositional gradients by the electrochemical codeposition of Au and Pd in the membrane to form an alloy that showed a continuous gradient in the Au/Pd ratio.[50] Hybrid polymer/metal NWs with a gradient in the length of the polymer were also fabricated. An in-plane potential gradient was used for the electrodeposition of polyaniline, which was followed by the electrodeposition of Ag or Cu.[51]

Another dynamic application of electrochemical gradients by the use of an in-plane potential gradient was shown by Yamada and Tada.[52] A charge gradient formed in a ferrocenyl-terminated alkanethiol monolayer by the application of an in-plane potential gradient gave a dynamically controlled wettability gradient.

2.2.1. *Bipolar Electrochemical Gradients*

A subclass of electrochemical gradients generated by an in-plane potential gradient is the bipolar electrochemical gradient. In contrast to the situation in Figure 2a, there are no conducting leads to either side of the bipolar electrode (Figure 3a), and the single bipolar electrode is both the anode and the cathode. Furthermore, there is a potential gradient in solution, whereas the bipolar electrode has a potential that is (roughly) equal everywhere on its surface. As a result,

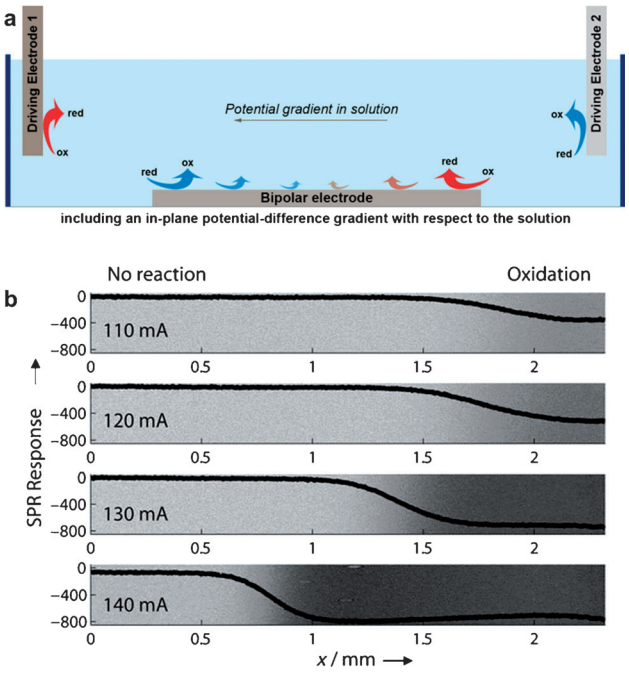

Figure 3. a) Creation, at a bipolar electrode, of an in-plane potential-difference gradient with respect to the solution by the use of a potential gradient in solution. A reactivity gradient (red arrows) of an electrochemical reaction is formed. b) SPR response, originating from a change in refractive index, of the anodic part of the bipolar electrode during the oxidation of $[Fe^{II}(CN)_6]^{4-}$ to $[Fe^{III}(CN)_6]^{3-}$ at different currents.[55] Copyright 2008, Wiley-VCH.

a potential difference is generated between the surface of the bipolar electrode and the solution, and this potential difference varies in-plane along the surface. When sufficient voltage is applied to an electrolyte solution containing a bipolar electrode, the potential difference between the bipolar electrode and the electrolyte solution drives electrochemical reactions, with the highest reaction rates at the edges of the bipolar electrode. Both 1D and 2D gradients can be fabricated with this method.[53] This section only focuses on the gradient-specific uses of bipolar electrochemistry. A more thorough description of this field can be found in two recent reviews.[54]

Björefors and co-workers used bipolar electrochemistry in 2008 for the fabrication of thiol gradients.[55] The potential-difference gradient used, which was induced by the solution potential gradient, was characterized by SPR by oxidizing $[Fe^{II}(CN)_6]^{4-}$ to $[Fe^{III}(CN)_6]^{3-}$ (Figure 3b). The position and width of the electrochemical gradient could be controlled, and the sigmoidal curves were explained by the logarithmic relationship between overpotential and the concentration ratio of $[Fe(CN)_6]^{3-}$ and $[Fe(CN)_6]^{4-}$. The fabricated thiol gradient consisted of a bicomponent gradient of methoxy-terminated and carboxylic acid terminated thiols. The carboxylic acid groups were used, after transformation into succinimide esters, to generate a protein (lysozyme) gradient. This setup was extended to the fabrication of radial gradients in thiol coverage by using an additional, pointed, Pt counter electrode positioned over the center of the bipolar electrode.[56]

Berggren and co-workers generated a wettability gradient by the fabrication of an oxidation gradient in a layer of conducting polyaniline doped with dodecylbenzenesulfonic acid as the active surface.[57] Fuchigami and co-workers fabricated conducting polymer films of poly(3-methylthiophene)[58] and other polymers[59] on ITO containing a gradient in electrochemical doping or chlorination. A conducting polymer of poly-3,4-(1-azidomethylethylene)dioxythiophene (PEDOT-N_3) was functionalized with a wettability or rhodamine gradient by click chemistry, by generating a gradient in the electrochemically generated Cu^+ catalyst.[60] A conducting fluorene-based polymer layer on boron-doped diamond (BDD) was used to carry out parallel reactions of a polymer that resulted in two functional polymers produced at the respective electrodes.[61] Furthermore, Shannon and co-workers fabricated Cd–S and Ag–Au alloy gradients by electrodeposition on a bipolar electrode,[62] whereas Sen and co-workers and Kuhn and co-workers created pH gradients by using bipolar electrochemistry.[63]

2.2.2. *Electrochemical Gradients Derived from an Asymmetric Electrode Configuration*

Another subclass of electrochemical gradients formed by an in-plane potential gradient is based on an asymmetric electrode configuration in the experimental setup (Figure 4a). The in-plane potential gradient on the working electrode is governed by the placement of the counter electrode. At positions further away from the counter electrode, there is a larger component of solution resistance, which lowers the applied potential at those positions, thus leading to a gradient in an electrochemical reaction.

Sailor and co-workers described in 2002 the use of this technique to electrochemically create a pore-size gradient in silicon.[64] The in-plane potential gradient resulted in a reactivity gradient for the electrochemical oxidation of Si in an HF solution in water/ethanol. In the same year, Arwin and co-workers demonstrated a similar method for the creation of a pore-size gradient on the back of a silicon wafer.[65] The same method was also used to fabricate nanoporous anodic alumina.[66]

Miskelly and co-workers fabricated gradients in the chemical modification of pore walls in thin-film porous silicon layers. By the electrochemical reduction of organohalides, gradients of methyl, pentyl acetate, and decyl groups covalently attached to silicon were formed.[67] Also, counter-propagating gradients of decyl groups in one direction and methyl groups in the other were fabricated by adjusting the position of the counter electrode after the first gradient was fabricated. Furthermore, 2D gradients were recently fabricated by combining a porous-silicon pore-size gradient (Figure 4b–i) with an orthogonal density gradient of a cyclic RGD peptide ligand.[68]

Macpherson and co-workers fabricated density and size gradients of Ag and Pt NPs electrodeposited on networks of single-walled carbon nanotubes (SWNTs).[69] They used a deposited Au strip at the edge of the SWNT substrate for contact, thus creating a potential drop in the SWNT network as a function of distance to the Au strip.

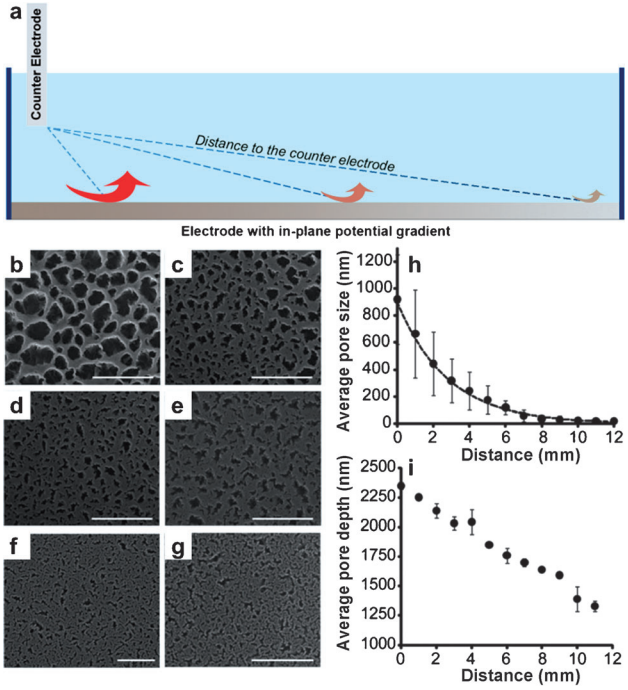

Figure 4. a) Creation of electrochemical gradients by the use of an asymmetric electrode-configuration. The in-plane potential gradient results in the reactivity gradient (red arrows) of an electrochemical reaction. b–g) SEM images showing a pore-size gradient in Si fabricated with an asymmetric electrode configuration: b) below the counter electrode, 0 mm (scale bar (sb) = 5 μm), c) 2 mm (sb = 5 μm), d) 6 mm (sb = 5 μm), e) 9 mm (sb = 2 μm), f) (sb = 200 nm), g) 12 mm (sb = 200 nm). h,i) Graphs of the average pore size (h) or pore depth (i) as a function of the distance to the counter electrode.[68] Copyright 2012, The Royal Society of Chemistry.

Larsen and co-workers employed this method for the fabrication of 2D monolayer surface gradients.[70] They used a Cu electrode as the anode, with a patterned insulating layer blocking the conduction path to the cathode in certain areas. As a cathode, an azide-terminated conductive polymer (PEDOT-N_3) was used. The varying distance to the anode gave a gradient in reduction of the inert Cu^{2+} to the catalytically active Cu^+, which was used for a click reaction of the azide with alkynylated molecules. Gradients of an alkyne functionalized with nitrilotriacetic acid (NTA) were used to capture His-tagged enhanced green fluorescent protein for visualization.

2.3. *Gradients Formed by the Combination of Electrochemistry with Other Methods*

2.3.1. *Gradients Created by Electrochemistry and Light*

The intensity of light can be applied in a gradient manner, for example, by using a photomask with a gradient pattern, to induce a chemical reaction that deprotects an electroactive layer (Figure 5a). Further electrochemical surface functionalization of the deprotected electroactive layer can then provide surface gradients.

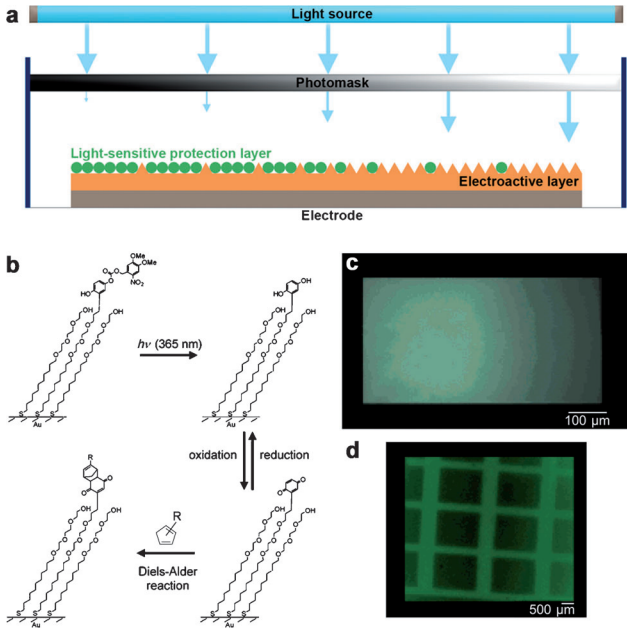

Figure 5. a) Creation of gradients by using a gradient in light intensity. The light deprotects an electroactive layer, on which further electrochemical surface functionalization is possible. b) Immobilization of fluorescein in patterns and gradients. Upon deprotection of a nitroveratryloxycarbonyl (NVOC)-protected hydroquinone by UV illumination, followed by electrochemical oxidation to the reactive quinone, fluorescein–cyclopentadiene is immobilized by Diels–Alder coupling. c,d) Fluorescence microscopy images: c) illumination through a gradient mask. d) sequential illumination through a mask with parallel lines (slits) in perpendicular orientations.[71] Copyright 2004, American Chemical Society.

Mrksich, Yousaf, and Dillmore developed this technique in 2004 for the immobilization of fluorescein in patterns and gradients (Figure 5b).[71] A photochemically active nitroveratryloxycarbonyl (NVOC)-protected hydroquinone monolayer was deprotected by UV illumination through a photomask to expose the redox-active hydroquinone in patterns and gradients. Subsequent electrochemical oxidation of the hydroquinone produced the quinone, which reacted with a fluorescein-modified cyclopentadiene derivative in a Diels–Alder coupling (Figure 5c,d). In a follow-up study, Yousaf and Chan used the quinone monolayer in combination with aminooxy-terminated ligands to form a stable oxime conjugate through chemoselective ligation, which resulted in ligand-density gradients on Au electrodes.[72]

In another case, a digital micromirror device was used to create a light pattern that generated conducting patches on a light-addressable electrode.[73] By using the conductive patches as a photoanode or -cathode and applying positive or negative voltages to generate protons or hydroxide ions, micron-scale pH gradients were generated. The gradients were formed around the conducting patches by diffusion.

2.3.2. *Gradients Created by Electrochemistry and Dip Coating*

A simple technique for the electrochemical fabrication of gradients is by the withdrawal of a substrate from a solution, for example, by draining the solution, while applying a potential (Figure 6a). This method effectively creates a gradient in reaction/deposition time as a function of position, thus resulting in a surface gradient.

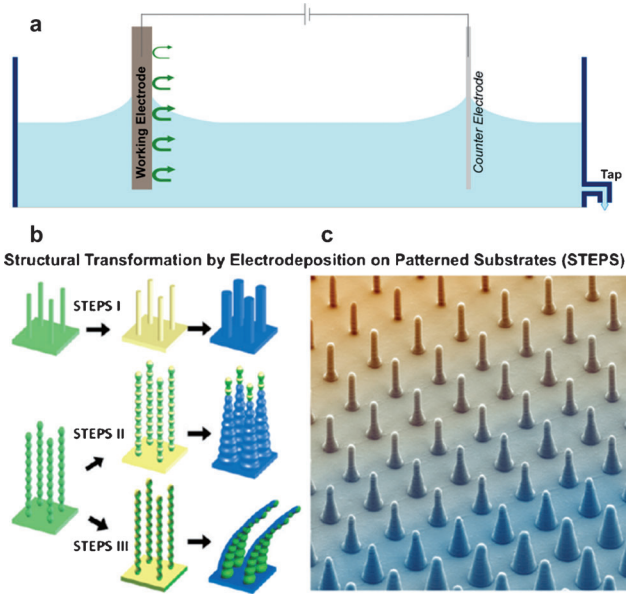

Figure 6. a) Electrochemical formation of gradients by the withdrawal of a substrate from a solution by draining the solution while applying a potential. b) Different fabrication methods of STEPS. The differences arise from the use of the techniques sputtering (I), evaporation (II), or evaporation at an angle (III). c) Gradient in the shape of the cones resulting from the combination of STEPS with dip coating.[75] Copyright 2011, American Chemical Society.

Encinas and co-workers used this method in 2011 to fabricate arrays of magnetic Ni nanowires with a gradient in length.[74] The gradient was formed by gradual withdrawal of a vertically positioned commercial porous anodized alumina (Al_2O_3) template with a thickness of 60 µm from the electrodeposition solution by draining the liquid with a syringe pump. Ni NWs were formed by electrodeposition only when in contact with the solution and thus exhibited a gradient in reaction time as a function of position, which resulted in a gradient in the length of the NWs.

In the same year, Aizenberg and co-workers created geometry gradients of high-aspect-ratio (HAR) structures of an electrodeposited conductive polymer. With this method, which was termed "structural transformation by electrodeposition on patterned substrates" (STEPS),[75,76] arrays of HAR nano- and microstructures could be transformed in terms of their size and shape. Different methods of evaporation gave different structures (Figure 6b). The combined use of dip coating led to a gradient in deposition time and thus, in combination with metal evaporation and scalloping, a gradient in the shape of the cones (Figure 6c). The formation of 2D gradients was possible by combining a gradient of the pitch between uniformly sized pillars in one direction with a gradient of the pillar diameter in the orthogonal direction. This method was extended to the

creation of gradients of concentric gold rings with controlled gap sizes.

Pesika and co-workers used this method to create a Ag roughness gradient by combining the withdrawal of a sample from a potassium silver cyanide solution with a changing overpotential of the whole electrode over time. The Ag roughness gradient was transferred into a gradient in roughness of polystyrene and polyurethane surfaces.[77]

2.3.3. Gradients Created by Electrochemistry and Magnetic Fields

The influence of magnetic fields on electrochemical processes is long-known,[78] but only recently has this technique been used to deposit structured Cu layers by the superposition of magnetic-field gradients.[79] Gradients were obtained by the application of a magnetic-field gradient perpendicular to the working electrode used for the electrodeposition of paramagnetic ions (Figure 7). The highest

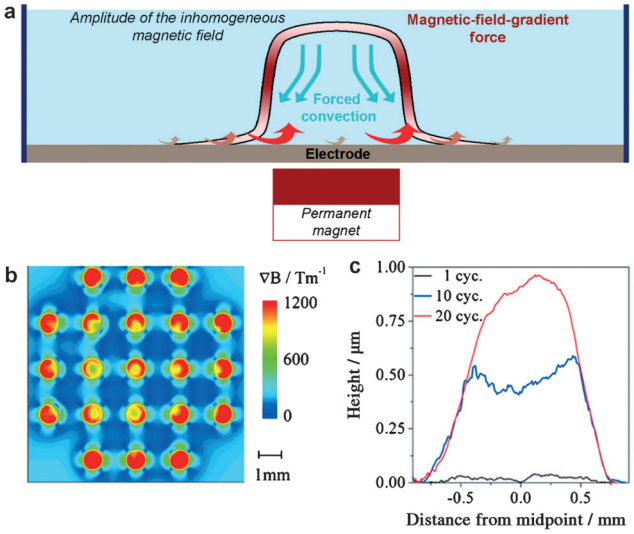

Figure 7. a) Creation of gradients by using magnetic-field gradients coupled with electrochemistry. Gradients in mass-transport-limited reactivity are obtained by electrolyte flow induced by the force of the magnetic-field gradient towards regions close to gradient maxima. b) Calculated distribution of the magnetic-field gradient. c) Profile plots of the central deposit after 1, 10, and 20 cycles.[81b] Copyright 2011, Elsevier.

amount of deposition was obtained close to the maxima of the magnetic-field gradients. The influence of a magnetic-field gradient on the electrodeposition of paramagnetic Cu^{2+} ions was proven to be governed by electrolyte flow induced by the force of the magnetic-field gradient towards regions close to the gradient maxima (see Figure 7a, red gradient).[80] This flow-enhanced transport of paramagnetic ions from the bulk electrolyte close to the gradient maxima increases the reactivity in mass-transport-limited reactions, such as Cu electrodeposition.[80] Coey and co-workers and Gebert and co-workers utilized this behavior in 2011 to fabricate Cu deposition gradients.[81] With this method, gradients from a few hundreds of microns up to the centimeter scale could be obtained.[80,81] An example in which Cu deposition gradients were obtained by pulse-reverse plating in a magnetic-field gradient is shown in Figure 7b,c. Figure 7b shows the calculated distribution of the magnetic-field gradient at the Au electrode. The template for the magnetic-field gradient consisted of 21 Fe wires embedded in poly(vinyl chloride). The profile plots of the central deposit in Figure 7c for 1, 10, and 20 cycles clearly show the gradient in Cu deposition. After one cycle, a thickness of almost 40 nm was measured.

Gebert and co-workers expanded this technique to diamagnetic ions, such as Bi^{3+}. Bi gradients were formed by adding electrochemically inert paramagnetic Mn^{2+} ions.[82] In this way it became possible to apply the method to almost every electrochemical system. A crucial difference with regard to the previous results, however, was that the deposited gradients were reversed with respect to the Cu gradients. This difference also originates from the increased electrolyte flow as a result of the magnetic-field gradient, although in this case the flow is directed away from the electrode in regions of high magnetic-field gradient, which reduces the deposition rate in those regions.[83]

3. Applications of Electrochemically Fabricated Gradients

Gradients have been used for a myriad of applications. Herein, we focus on the application of gradients fabricated by purely electrochemical methods or by electrochemistry in combination with other methods. Biological applications are discussed first, and then technological applications. A focus lies on the areas of high-throughput screening, (electro)-deposition, cell-migration studies, the addition of functionality to devices, and the driving of motion.

3.1. Biological Applications

3.1.1. High-Throughput Screening and Deposition

One of the most well-known applications of static gradients is high-throughput screening, for example, in materials science,[12] biomaterials,[10] and sensing materials.[14] Static gradients are often applied for biological applications in the screening of parameters that influence cell adhesion, cell morphology, and downstream signaling processes.[10,22b,24a,84] Electrochemically generated gradients are used for these purposes. Gradients in carboxylic acid terminated self-assembled monolayers (SAMs), after functionalization with fibronectin (FN), have been used to study cell adhesion.[41a] Gradients in Au topography on glass and a gradient in the density of hexadecanethiol SAM have been used for the same purpose.[36]

More elaborate studies have been performed with gradients in topography, in particular, the use of pore-size gradients. By using a pore-size gradient in Si, cell density and morphology were studied as a function of topography.[85] Besides cell density and morphology, the number of cell–cell interactions was also studied by using a similar pore-size gradient in alumina.[66] Furthermore, 2D gradients combining a pore-size gradient in Si with an RGD-ligand-density

gradient were used to probe two parameters pertaining to cell density at the same time.[68]

Recently, Malliaras and co-workers used the in-plane-potential-gradient method, applied to an ITO/conductive-polymer hybrid, to gain electrical control over protein conformation.[86] By the use of Förster resonance energy transfer (FRET), the conformation of FN was characterized to be compact and partially unfolded for high and low FRET ratios, respectively. The results show a gradient in FN conformation, from compact to partially unfolded (Figure 8a). This control over the conformation of FN was used to compare cell-adhesion behavior. A 60% higher cell density was found on an oxidized patch. This finding was correlated with the well-established integrin binding model, according to which two of the peptide sequences of FN should be in close proximity for efficient binding to occur.

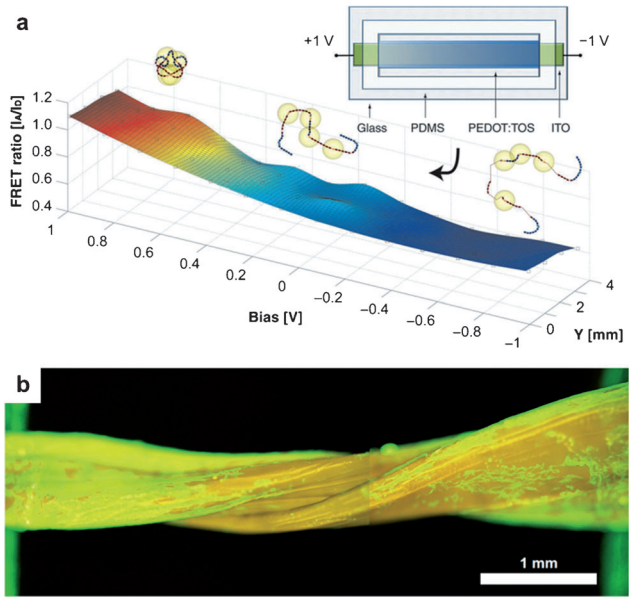

Figure 8. a) Gradually changing FN conformation along a surface with an in-plane potential gradient, as shown by the FRET ratio as a function of applied potential (PEDOT:TOS is PEDOT doped with tosylate).[86] Copyright 2012, Wiley-VCH. b) Fluorescence microscopy image of three intertwined, oriented collagen bundles stained with Alexa-Fluor 488 Phalloidin, showing the migration and proliferation of tendon-derived fibroblasts.[28a] Copyright 2008, Elsevier.

Another well-known application of gradients is high-throughput deposition. pH gradients created by the electrolysis of water or other chemical reactions (electrochemical reduction of *p*-benzoquinone or H_2O_2) are a prime example of gradients used for the deposition of materials. The working mechanism is most often pH-triggered precipitation. Many biologically relevant polymers have been deposited, such as chitosan,[31,87] alginate,[88] and agarose.[88b] For an in-depth overview of the deposition of biologically relevant polymers, the reader is referred to several reviews.[89] Molecular gelators, such as 9-fluorenylmethoxycarbonyl (Fmoc) amino acids, Fmoc-peptides,[90] and Fmoc-dipeptides,[91] can also be deposited by this method with spatial control of the deposition in normal and lateral directions. Furthermore, pH gradients have been used to induce the controlled assembly of collagen molecules, which could even be aligned in highly oriented and densely packed elongated bundles.[28a] These collagen bundles were beneficial for cell proliferation and imposed their orientation on the tendon cells (Figure 8b).

3.1.2. Cell-Migration Studies

Static gradients are used to study cell migration. Endothelial cell migration on surfaces was studied by Jiang and coworkers,[41b] who employed thiol gradients obtained by an in-plane potential gradient. Proteins were covalently immobilized through their amino groups on activated esters by activating a backfilled COOH-terminated thiol gradient with *N*-hydroxysuccinimide/EDC to fabricate gradients of FN, vascular endothelial growth factor (VEGF), or a combination thereof. Cell-displacement rates were compared on different surfaces with gradients of three different compositions and two different degrees of steepness. It was found that for the size range studied (approximately the millimeter range), the gradient steepness did not play a role. The surface with a combination of FN and VEGF displayed the largest displacement.

Yousaf and Chan used a system which combined light and electrochemistry to fabricate ligand patterns and gradients in ligand density on Au.[72] RGD-peptide-density gradients were used to investigate the ligand density needed to support cell adhesion along the gradient. Differences for high/low cell seeding were found, as well as a dependence on the slope of the gradient (Figure 9). For steeper slopes, higher ligand densities were necessary to support cell adhesion. Factors that influence and regulate cell polarity were also investigated. Cells were found to polarize consistently in the higher-density direction, except at high cell densities, when the cell–cell interactions dominated the ligand gradient.

Because the dynamic processes in biological systems are for a large part governed by spatiotemporal concentration gradients on a surface or in solution, methods to investigate this behavior should be able to mimic the spatiotemporal behavior. Many cells employ such processes, for example, leukocytes during inflammatory responses, and neuronal and embryonic cells during development, and such processes also play a role in certain types of cancer.[92] The use of artificial methods to generate such gradients may give insight into the intercellular and extracellular processes that govern cell motility and cell–cell communication, and may lead to applications in tissue engineering.[72] In the simplest form of such a method, cell adhesion is turned on and off on a dynamic surface.[84,93] A short and select overview focused on electrochemistry is given herein. For a more general overview of all the different methods and uses of dynamic substrates for cell studies, the reader is referred to two recent reviews.[94]

One of the most common approaches to the use of electroactive substrates for cell studies is the changing of ligand density in space or in an on/off manner. For example, Mrksich and Yousaf used quinone-terminated monolayers, which were formed by electrochemical oxidation of the hydroquinone, to immobilize proteins with a cyclopentadiene group by a Diels–Alder reaction.[95] This method was

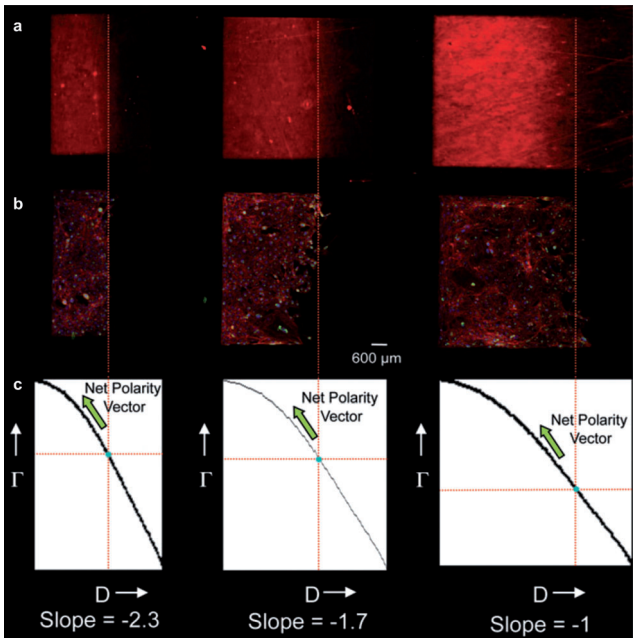

Figure 9. Determination of the ligand density needed for cell adhesion and the effect on cell polarization for different RGD-peptide gradients. a) Fluorescence microscopy images of an immobilized oxyamine–rhodamine gradient. b) Fluorescence microscopy images of cell cultures attached to RGD immobilized gradients. For high cell-seeding density, cell adhesion is dependent on the gradient slope and density of the RGD peptide. c) Plots of relative ligand density versus distance (D is distance in (a–c) in μm, and Γ is ligand density). For higher gradient slopes, a higher ligand density is necessary for cell adhesion.[72] Copyright 2008, The Royal Society of Chemistry.

extended to include the option of electrochemically releasing the ligand by reduction to the hydroquinone.[95] By electrochemically promoting the release or adhesion of an RGD peptide, this system was used to selectively release adherent cells from the surface; in this way, cell migration was turned on.[96] Furthermore, a combination of the two methods was reported:[97] Cells were released from parts of the surface by the release of an RGD ligand by electrochemical oxidation. Cell migration was switched on by treating the resulting quinone with a cyclopentadiene-tagged RGD peptide in a Diels–Alder reaction. This system was also used to pattern the cell adhesion of two different cell populations.[98]

Yousaf and Chan used an electroactive system that deviated slightly from the previously described system.[99] The same (hydro)quinone SAM, in which the quinone is reactive, whereas the hydroquinone is not, was used, now with the subsequent coupling of an aminooxy derivative to give an oxime. The biggest advantage of this method is that both the oxime and the quinone are electroactive, which makes it possible to determine the yield of the reaction in a controlled manner in real time.[99] By combining this system with microfluidic depletion and different surface-exposure times, a gradient in the density of an oxyamine-terminated RGD peptide was fabricated. In combination with microcontact printing (μCP) of hexadecanethiol (HDT), which formed a "starting" cell-adhesive patch after FN physisorption, spatial and temporal (on/off) control over cell migration was achieved.[35] This system was used to study the influence of the direction of the surface gradient on haptotactic migration. Cells only attached to and proliferated on the HDT patch covered with FN before activation of the hydroquinone gradient, which intersected the HDT patch. After oxidation, which created a quinone gradient, and the immobilization of the oxyamine-terminated RGD peptide, the migration was turned on, and cells were found to migrate along the gradient, towards the higher density of RGD.

The hydroquinone system was also combined with a light-sensitive protecting group (NVOC), which gave the system dual functionality and provided a straightforward method of patterning the electrochemically active regions.[71] Yousaf and co-workers developed this system further and showed how a dynamic, reversible electroactive substrate was able to immobilize ligands, proteins, and cells in patterns and gradients and later release them.[100] The same chemical system of the electroactive quinone SAM was used in combination with oxyamine ligands. UV illumination deprotected the NVOC groups to reveal patterns and gradients of the hydroquinone, which could be oxidized to the quinone functionality. The addition of an oxyamine-terminated RGD ligand led to an oxime conjugate, thus rendering the surface cell-adhesive. Several immobilization and release steps could be repeated, thus resulting in a switchable and reusable system.

This system was used to probe the influence of haptotactic gradients, especially their direction and steepness, on the migration speed of cells.[101] The cells were confined to cell-adhesive patches created by μCP, and in a gradient manner, the NVOC groups were removed in two dumbbell-shaped patterns, which were positioned across the two patches. The two gradients had different degrees of steepness (the left-hand gradient was steeper). After the oxidation and immobilization of oxyamine-terminated RGD, the gradients were switched to the cell-adhesive mode, and cell migration was studied (Figure 10a). Migration was investigated without (D), up (B, F), or down (A, C, E, G) the gradient, and zones were set from 0 to 100% (Figure 10b). The results of the migration study are shown in Figure 10c, in which the migrated distance is plotted as a percentage versus time. The fastest migration was found on the steeper gradient, both up and down the gradient. Overall, the cells migrated faster down the gradient than up the gradient.

3.2. Technological Applications

3.2.1. High-Throughput Screening

There are also many examples of technological applications of static gradients for high-throughput screening. Hillier and Jayaraman used electrochemical gradients as early as 2001 for catalyst discovery and characterization.[46] A gradient in Pt coverage was created by the use of an in-plane potential gradient on an ITO surface. This catalyst gradient was characterized by scanning electrochemical microscopy (SECM) in combination with a noncatalytic redox probe. A uniformly reactive surface was found. However, imaging with a catalytic redox probe showed variations in reactivity toward

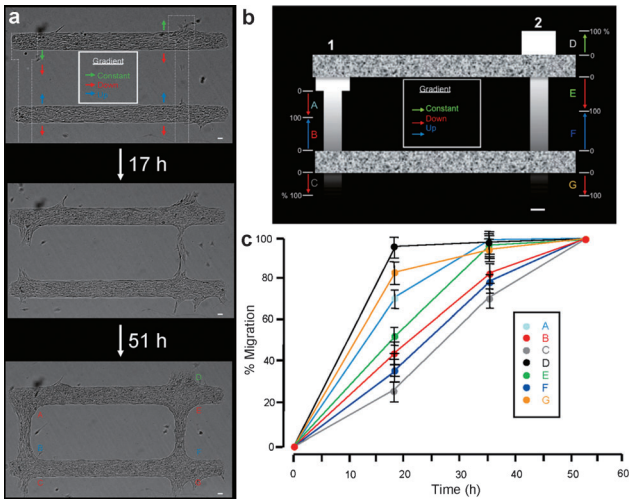

Figure 10. a) Time-lapse microscopy images used for the investigation of the influence of gradient direction and steepness on the migration speed of cells. Two dumbbell-shaped gradients of RGD ligands with different slopes were positioned across two parallel cell-adhesive patches created by μCP. After RGD-ligand immobilization, cells migrated up and down the two gradients (sb = 100 μm). b) Schematic overview of the two gradients positioned across the two patches. Zones of migration were defined as without (D), up (B, F), or down (A, C, E, G) the gradient (sb = 200 μm). c) Graph showing the migrated distance as a percentage versus time for each zone.[101] Copyright 2011, American Chemical Society.

the hydrogen oxidation reaction on the surface. Furthermore, by using an in-plane potential gradient combined with a homogeneous-catalyst (Pt) layer, several electrochemical reactions were investigated as a function of potential, such as the oxidation of $[Ru(NH_3)_6]^{2+}$ and H_2, the latter in the absence and presence of adsorbed CO.[102]

A closely related set of studies based on the use of bipolar electrochemistry was reported from 2002 onward by Crooks and co-workers. From a practical perspective, bipolar electrochemistry is convenient, as electrical leads to the electrodes in solution are not needed, which makes scaling up for high-throughput screening a lot easier. Direct optical readout of the electrochemical reactions was also possible on the basis of the electrogenerated chemiluminescence (ECL) of $[Ru(2,2'\text{-bipyridine})_3]^{2+}$, which was chemically decoupled from, but electrically coupled to, the electrochemical sensing reaction.[103] Because of the in-plane potential gradient and the fact that the bipolar electrode acts as both an anode and a cathode, the illuminated length of the electrode is a function of the formal potential of the half-reaction under study. This method was modified to use the electrodissolution of Ag as a reporter reaction instead of ECL.[104] Thus, the result, that is, the shortening of the Ag microband, was permanent, and it could be read out by the naked eye or with a magnifying glass. Also, the sensitivity and limit of detection of the method could be adjusted by changing the cross-sectional area of the Ag microband.

The reporting by electrodissolution of Ag was used for the screening of electrocatalyst candidates for the oxygen reduction reaction (ORR).[105] As a proof of principle, Pt, ITO and Au were compared, and a direct relationship between the activity of the electrocatalyst and the number of dissolved Ag microbands was shown. More recently, electrocatalysts were compared by this method in parallel experiments by preparing 11 distinct compositions of three bimetallic electrocatalysts (Pd-M, in which M = Au, Co, W).[106] Cr instead of Ag microbands were used to reduce the risk of poisoning of the catalysts. Figure 11a shows optical microscopy images of a bipolar electrode before and after such a screening experiment. The red stripes indicate the final number of Cr microbands removed for the different compositions of Pd–Co; this number is related to the onset potential of the ORR. Thus, the different compositions could be reliably compared and evaluated.

The in-plane potential gradient created by an asymmetric electrode configuration was used by Macpherson and co-workers to fabricate gradients in the density and size of Ag NPs on SWNT networks.[107] These gradients were used for the investigation and optimization of surface enhanced Raman scattering (SERS) as a function of NP size and density. An in-plane potential gradient formed by bipolar electrochemistry was used by Shannon and Ramaswamy to fabricate Ag–Au alloy gradients on stainless steel.[62b] These gradients were screened for the maximum SERS intensity,

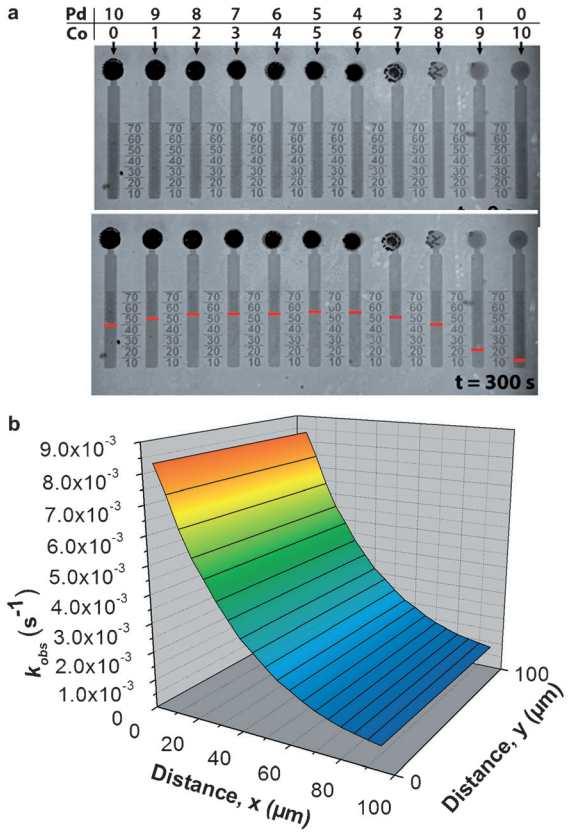

Figure 11. a) Optical microscopy images showing the number of Cr microbands removed by different compositions of Pd–Co. The red stripes indicate the final number of Cr microbands removed.[106] Copyright 2013, American Chemical Society. b) A 3D reactivity map of the e-click reaction kinetics showing the k_{obs} values mapped in space between the two electrodes.[33]

which occurred at 100% Ag and at an alloy composition of 70% Ag/30% Au.

Recently, our research group used electrochemically generated solution gradients to study the efficiency of surface reactions in a highly parallel manner.[33] Electrochemically derived solution gradients of a reaction parameter (pH) and a catalyst (Cu^{+}) were used to fabricate surface gradients on the micron scale and to study the kinetics of (surface-confined) imine hydrolysis and the copper(I)-catalyzed azide–alkyne 1,3-dipolar cycloaddition, respectively. A 3D reactivity map of the e-click reaction kinetics is shown in Figure 11b. By combining experimental and modeling data, the reaction order of the click reaction in the Cu^{I} catalyst was deduced (second-order dependence on Cu^{I}).

3.2.2. *High-Throughput Deposition*

Aizenberg and co-workers developed two methods for high-throughput deposition. One system consisted of a microfluidic gradient of a reaction parameter in combination with electrochemical deposition. It was used to identify the conditions that govern the morphology of the resulting electrodeposited polypyrrole (PPy).[108] By varying the concentration of the pyrrole monomer, PBS, and the pH value, the deposition conditions were optimized to produce PPy surfaces with a high surface area and a large scattering and absorption cross-section or with superhydrophobic properties. The second method was STEPS, as discussed in Section 2.3.2.[75] Several applications of this method were shown, including its combination with nanoskiving to create ordered periodic arrays of metallic concentric rings, so-called ring resonators, with a gradient in gap size (Figure 12a,b). Also, the spontaneous patterning of rod-shaped bacteria was investigated by fabricating a surface exhibiting a range of HAR structures with variable pitch, post diameter, and gap width (Figure 12c,d).[75,109]

High-throughput deposition has also been performed on particles. Oscarsson and co-workers reported the fabrication of many micron-sized particles with one or multiple functionalized patches,[110] but also Au and protein gradients.[34] Kuhn and co-workers reported a high-throughput method of fabricating Janus particles, mostly on the hundreds-of-microns scale, by bipolar electrochemistry.[63b] When an in-plane potential gradient was used on a single particle, two different electrochemical reactions could take place on either side of the particle. The pH gradient achieved by electrolysis of water on opposite sides of the particle, for example, could be used for controlled polymerization or precipitation. This approach was used in sol–gel processes to deposit silica, silicone, and TiO_2, but also to deposit organic layers, such as paints (by electrophoretic deposition), on one side of a glassy-carbon particle. The method was extended further to smaller, micron-sized particles and wires, on which metals (Au, Ag) were deposited.[111] Other applications of high-throughput deposition consist of the electrodeposition of Au–Pd in gradients to create NWs with a continuously changing Au–Pd alloy composition.[50]

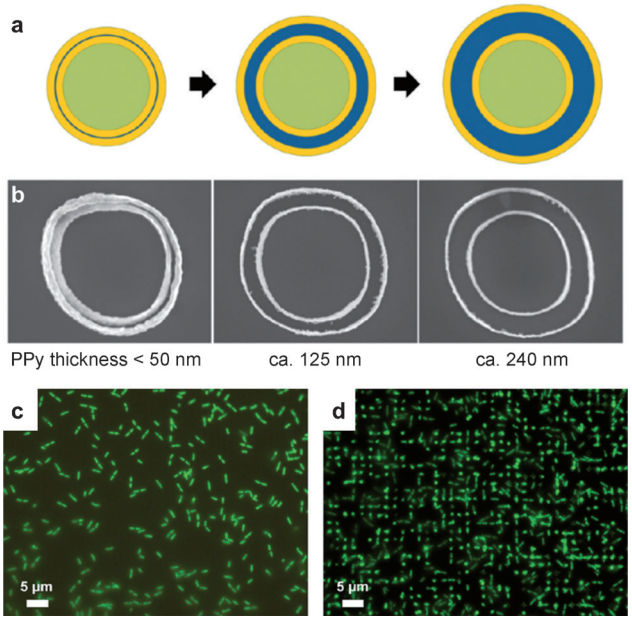

Figure 12. a) Schematic illustration of the creation of different ring resonators exhibiting a gradient in gap size (green: core epoxy parent structure; yellow: sputter-coated gold; blue: PPy). b) SEM images of a sample with ring resonators exhibiting a gradient in gap size. c,d) Fluorescence microscopy images of spontaneous bacterial patterning on a surface exhibiting a gradient in the interstitial space between HAR nanopillars. No bacterial patterning was observed with a large interstitial space (c), whereas patterning occurred on widened pillars with a smaller interstitial space (d).[75] Copyright 2011, American Chemical Society.

3.2.3. *Driving Motion*

Static gradients can drive motion, for example, of liquid droplets. Berggren and co-workers showed liquid motion on static wettability gradients fabricated by the use of an in-plane potential gradient.[57] The working principle is based on the large differences in the water contact angle between an oxidized and reduced surface of conducting polyaniline doped with dodecylbenzenesulfonic acid.

Dynamic gradients have clear advantages over static gradients for controlling liquid motion, because they open up the option of controlling the motion in space and time. Abbott and co-workers used dynamic gradients, fabricated by electrochemistry and diffusion, of surface-active species ((11-ferrocenylundecyl)trimethylammonium) to control the motion and position of aqueous and organic liquids.[26] The motion of droplets of a nematic liquid crystal (LC, 4-*n*-pentyl-4′-cyanobiphenyl) could be dynamically controlled in microchannels, in the direction of the oxidizing electrode and away from the reducing electrode (Figure 13a,b). Furthermore, sulfur microparticles floating on top of a solution containing surface-active species could be controllably moved away from the reducing electrodes (Figure 13c). By changing the potential at different points in time, the direction and speed could be adjusted (Figure 13d). Tada and Yamada used electrochemically controlled in-plane potential gradients to generate a dynamic wettability gradient that enabled the movement of

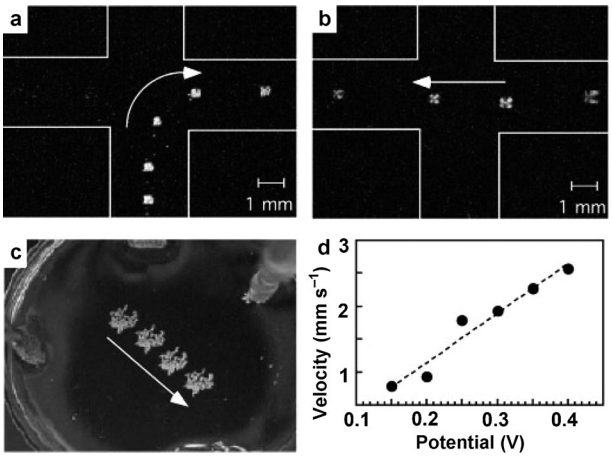

Figure 13. Time-lapse images (ca. 0.5 Hz) showing dynamic control of the motion of LC droplets within a microfluidic network. a) The LC droplet originates from the bottom; the right channel has a potential of 0.3 V and the bottom channel a potential of −0.3 V versus SCE. b) The LC droplet originates from the right; the right channel has a potential of −0.3 V and the left channel a potential of 0.3 V versus SCE. c) Time-lapse image (ca. 0.3 Hz) of the controlled motion of sulfur microparticles floating on top of a solution containing surface-active species, away from the reducing left and top Pt electrodes. d) Graph of the velocity of the droplet versus the applied potential of the anode and cathode.[26] Copyright 1999, AAAS.

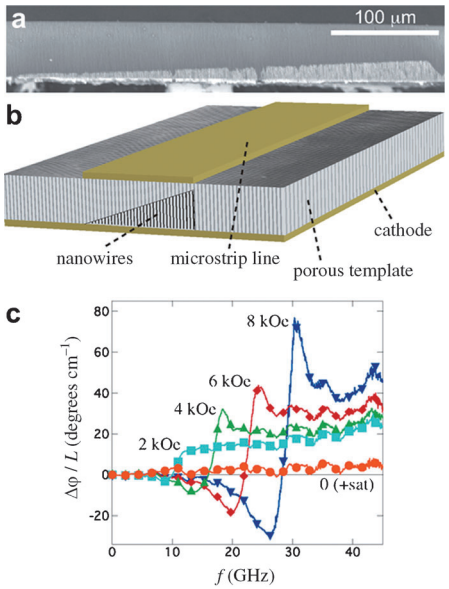

Figure 14. a) SEM image of a 390 μm wide NW array with a gradient in NW length. b) Schematic representation of a nonreciprocal microstrip line. c) Graph showing the differential phase shift of the nonreciprocal microstrip line.[74] Copyright 2011, American Chemical Society.

nitrobenzene, dichloromethane, and hexadecane droplets in a controllable manner.[52] The gradient could be varied by moving the position of the $E_{1/2}$ potential of Fc (ferrocene) on the surface by changing the applied offset voltage and the total applied potential gradient. Furthermore, a rudimentary method to manipulate microparticles was shown in which the moving droplet pushed glass beads with a size of 40 μm.

3.2.4. *Towards Devices*

Several reports describe the fabrication of gradients for device development. In 2002, Sailor and co-workers showed the electrochemical fabrication of a pore-size gradient in Si by using an asymmetric electrode configuration, and its use as a size-exclusion matrix in the determination of the size of proteins.[64] The same research group also demonstrated pH-controlled protein gating, whereby detection was performed by optical-reflectivity measurements. A rugate optical filter with a gradient in rejection-band wavelengths was fabricated,[112] as well as an ethanol sensor for aqueous solutions based on a gradient in the chemical modification of pore walls in thin-film porous silicon layers.[67]

Encinas and co-workers developed a microwave phase shifter with improved microwave nonreciprocal behavior by fabricating a nonreciprocal microstrip line containing a gradient in the length of magnetic Ni NWs through simultaneous electrodeposition and dip coating.[74] The gradient in NW length (Figure 14a,b) effectively created a gradient in permittivity along the width of the microstrip. This device displayed improved behavior (Figure 14c) as compared to a device with an asymmetrical arrangement of NW lengths in a stairwaylike profile.

4. Summary and Outlook

In the last 10 to 15 years there has been tremendous development in the field of gradients fabricated by the use of electrochemistry. New methods have been developed, from purely electrochemical methods, such as the use of diffusion-based systems or in-plane potential gradients, to the combination of electrochemistry with other methods, such as the use of light and magnetic fields. In terms of their application, electrochemically fabricated gradients have also shown considerable progress. They are used extensively for biological applications, for example, for the high-throughput screening of parameters that influence cell adhesion and morphology, and for the high-throughput deposition of responsive, film-forming biopolymers and molecular gelators. They also have many technological applications, for example, in the high-throughput screening of catalysts, in high-throughput deposition, for the optimization of deposition conditions, and for the fabrication of Janus particles. Such gradients are also being used for device development and for driving motion, such as that of liquid droplets.

Most described applications use static gradients; however, a trend is emerging towards the use of dynamic gradients. The dynamic nature of these gradients plays a crucial role, as it enables the spatiotemporal probing of processes or control over processes. The use of spatial and temporal control over electrochemical gradients is still in its infancy. A few very interesting and promising studies have been reported recently that show the flexibility and power of this control. Such control has allowed the investigation of the influence of haptotactic gradients, and in particular their direction and steepness, on the motility of cells, for example, or on the controlled and directional driving of liquid-droplet motion.

We envision that the spatial and temporal control of electrochemical gradients in the millimeter-to-centimeter size range will be used for applications of droplet motion, for example, in nanochemistry. In this size range, in-plane gradients are of particular interest. The temporal and spatial control of micron-sized gradients enables cell interactions, migration (haptotaxis, chemotaxis), and other characteristics to be probed in ensembles and on the single-cell level,[25,101] especially in health-related systems, such as angiogenesis and wound healing, or in certain types of cancer.[92] A very interesting development is the extension of these methods to the production of gradients inside cells,[8,9,113] with the potential to probe or affect a variety of cellular processes.[4] In this size range, electrochemical gradients created by the in-plane-potential-gradient and diffusion methods are applicable. Besides the powerful electroactive SAMs described herein, it would be interesting to see some newly developed electroactive SAMs (for example, electroactive supramolecular SAMs of β-cyclodextrin[114] and cucurbiturils,[115] or other reversible electroactive layers[116]), which have been used for the reversible attachment of proteins, peptides, and cells, combined with in-plane potential gradients. Furthermore, it is envisioned that temporal and spatial control of micro/nanometer-sized gradients could be used for the controlled and directed motion of nanoobjects, such as NPs,[117] nanocontainers (e.g. virus capsids), and single molecules, for example, in nanochemistry and nanolocomotion. In this case, the methods for creating electrochemical gradients must also be developed further. For example, the diffusion method and the coupling of electrochemistry with light hold the potential for the fabrication of gradients on the sub-micrometer scale. Overall, this Review has dealt with both established and new methods of electrochemical gradient formation. These methods have paved the way for the development of a myriad of new applications. Especially promising are the developments towards the investigation of dynamic phenomena, which is expected to have a bright future.

Maaike Heitink is gratefully acknowledged for designing the schematic images in Section 2. Cover art has been designed by Tjeerd Willem Droogers. This work was supported by the Council for Chemical Sciences of the Netherlands Organization for Scientific Research (NWO-CW, Vici grant 700.58.443 to J.H.).

Received: November 28, 2013
Published online: June 24, 2014

[1] M. Weber, R. Hauschild, J. Schwarz, C. Moussion, I. de Vries, D. F. Legler, S. A. Luther, T. Bollenbach, M. Sixt, *Science* **2013**, *339*, 328.

[2] a) M. Ueda, Y. Sako, T. Tanaka, P. Devreotes, T. Yanagida, *Science* **2001**, *294*, 864; b) P. J. M. Van Haastert, P. N. Devreotes, *Nat. Rev. Mol. Cell Biol.* **2004**, *5*, 626; c) G. Servant, O. D. Weiner, P. Herzmark, T. Balla, J. W. Sedat, H. R. Bourne, *Science* **2000**, *287*, 1037.

[3] B. G. Fuller, M. A. Lampson, E. A. Foley, S. Rosasco-Nitcher, K. V. Le, P. Tobelmann, D. L. Brautigan, P. T. Stukenberg, T. M. Kapoor, *Nature* **2008**, *453*, 1132.

[4] B. N. Kholodenko, J. F. Hancock, W. Kolch, *Nat. Rev. Mol. Cell Biol.* **2010**, *11*, 414.

[5] a) N. I. Markevich, M. A. Tsyganov, J. B. Hoek, B. N. Kholodenko, *Mol. Syst. Biol.* **2006**, *2*, 61; b) H. Meinhardt, A. Gierer, *Bioessays* **2000**, *22*, 753; c) S. R. Neves, P. Tsokas, A. Sarkar, E. A. Grace, P. Rangamani, S. M. Taubenfeld, C. M. Alberini, J. C. Schaff, R. D. Blitzer, I. I. Moraru, R. Iyengar, *Cell* **2008**, *133*, 666.

[6] a) O. Brandman, T. Meyer, *Science* **2008**, *322*, 390; b) Q. A. Justman, Z. Serber, J. E. Ferrell, H. El-Samad, K. M. Shokat, *Science* **2009**, *324*, 509.

[7] a) C. Wu, S. B. Asokan, M. E. Berginski, E. M. Haynes, N. E. Sharpless, J. D. Griffith, S. M. Gomez, J. E. Bear, *Cell* **2012**, *148*, 973; b) N. L. Jeon, H. Baskaran, S. K. W. Dertinger, G. M. Whitesides, L. Van De Water, M. Toner, *Nat. Biotechnol.* **2002**, *20*, 826; c) J. Wu, X. Wu, F. Lin, *Lab Chip* **2013**, *13*, 2484.

[8] Y. I. Wu, D. Frey, O. I. Lungu, A. Jaehrig, I. Schlichting, B. Kuhlman, K. M. Hahn, *Nature* **2009**, *461*, 104.

[9] a) A. Levskaya, O. D. Weiner, W. A. Lim, C. A. Voigt, *Nature* **2009**, *461*, 997; b) C. Hoffmann, E. Mazari, S. Lallet, R. Le Borgne, V. Marchi, C. Gosse, Z. Gueroui, *Nat. Nanotechnol.* **2013**, *8*, 199.

[10] C. G. Simon, S. Lin-Gibson, *Adv. Mater.* **2011**, *23*, 369.

[11] a) T. P. Kunzler, T. Drobek, M. Schuler, N. D. Spencer, *Biomaterials* **2007**, *28*, 2175; b) C. Zink, H. Hall, D. M. Brunette, N. D. Spencer, *Biomaterials* **2012**, *33*, 8055.

[12] W. F. Maier, K. Stöwe, S. Sieg, *Angew. Chem.* **2007**, *119*, 6122; *Angew. Chem. Int. Ed.* **2007**, *46*, 6016.

[13] a) S. Jayaraman, A. C. Hillier, *J. Comb. Chem.* **2004**, *6*, 27; b) S. Jayaraman, A. C. Hillier, *Meas. Sci. Technol.* **2005**, *16*, 5.

[14] R. A. Potyrailo, V. M. Mirsky, *Chem. Rev.* **2008**, *108*, 770.

[15] R. B. van Dover, L. F. Schneemeyer, R. M. Fleming, *Nature* **1998**, *392*, 162.

[16] a) M. K. Chaudhury, G. M. Whitesides, *Science* **1992**, *256*, 1539; b) S. Daniel, M. K. Chaudhury, J. C. Chen, *Science* **2001**, *291*, 633.

[17] K. Ichimura, S.-K. Oh, M. Nakagawa, *Science* **2000**, *288*, 1624.

[18] T. Chang, D. I. Rozkiewicz, B. J. Ravoo, E. W. Meijer, D. N. Reinhoudt, *Nano Lett.* **2007**, *7*, 978.

[19] P. Burgos, Z. Zhang, R. Golestanian, G. J. Leggett, M. Geoghegan, *ACS Nano* **2009**, *3*, 3235.

[20] A. Perl, A. Gomez-Casado, D. Thompson, H. H. Dam, P. Jonkheijm, D. N. Reinhoudt, J. Huskens, *Nat. Chem.* **2011**, *3*, 317.

[21] S. Morgenthaler, C. Zink, N. D. Spencer, *Soft Matter* **2008**, *4*, 419.

[22] a) J. Genzer, R. R. Bhat, *Langmuir* **2008**, *24*, 2294; b) M. S. Kim, G. Khang, H. B. Lee, *Prog. Polym. Sci.* **2008**, *33*, 138; c) X. Lin, Q. He, J. Li, *Chem. Soc. Rev.* **2012**, *41*, 3584; d) J. Genzer, *Annu. Rev. Mater. Res.* **2012**, *42*, 435.

[23] N. L. Jeon, S. K. W. Dertinger, D. T. Chiu, I. S. Choi, A. D. Stroock, G. M. Whitesides, *Langmuir* **2000**, *16*, 8311.

[24] a) T. M. Keenan, A. Folch, *Lab Chip* **2008**, *8*, 34; b) S. Kim, H. J. Kim, N. L. Jeon, *Integr. Biol.* **2010**, *2*, 584.

[25] B. Meier, A. Zielinski, C. Weber, D. Arcizet, S. Youssef, T. Franosch, J. O. Rädler, D. Heinrich, *Proc. Natl. Acad. Sci. USA* **2011**, *108*, 11417.

[26] B. S. Gallardo, V. K. Gupta, F. D. Eagerton, L. I. Jong, V. S. Craig, R. R. Shah, N. L. Abbott, *Science* **1999**, *283*, 57.

[27] a) S. Fiedler, R. Hagedom, T. Schnelle, E. Richter, B. Wagner, G. Fuhr, *Anal. Chem.* **1995**, *67*, 820; b) K. Macounová, C. R. Cabrera, M. R. Holl, P. Yager, *Anal. Chem.* **2000**, *72*, 3745; c) S. M. Mitrovski, R. G. Nuzzo, *Lab Chip* **2005**, *5*, 634; d) D. Kohlheyer, J. C. T. Eijkel, S. Schlautmann, A. van den Berg, R. B. M. Schasfoort, *Anal. Chem.* **2007**, *79*, 8190; e) C. Nicosia, S. O. Krabbenborg, D. N. Reinhoudt, J. Huskens, *Supramol. Chem.* **2013**, *25*, 756.

[28] a) X. Cheng, U. A. Gurkan, C. J. Dehen, M. P. Tate, H. W. Hillhouse, G. J. Simpson, O. Akkus, *Biomaterials* **2008**, *29*, 3278; b) N. G. Weiss, M. A. Hayes, A. A. Garcia, R. R. Ansari, *Langmuir* **2011**, *27*, 494.
[29] C. Nicosia, S. O. Krabbenborg, P. Chen, J. Huskens, *J. Mater. Chem. B* **2013**, *1*, 5417.
[30] B. Li, B. Yu, W. T. S. Huck, W. Liu, F. Zhou, *J. Am. Chem. Soc.* **2013**, *135*, 1708.
[31] Q. Zhou, Q. Xie, Y. Fu, Z. Su, X. Jia, S. Yao, *J. Phys. Chem. B* **2007**, *111*, 11276.
[32] J. van Weerd, S. O. Krabbenborg, J. Eijkel, M. Karperien, J. Huskens, P. Jonkheijm, *J. Am. Chem. Soc.* **2014**, *136*, 100.
[33] S. O. Krabbenborg, C. Nicosia, P. Chen, J. Huskens, *Nat. Commun.* **2013**, *4*, 1667.
[34] K. Eriksson, P. Palmgren, L. Nyholm, S. Oscarsson, *Langmuir* **2012**, *28*, 10318.
[35] B. M. Lamb, N. P. Westcott, M. N. Yousaf, *ChemBioChem* **2008**, *9*, 2628.
[36] N. P. Westcott, B. M. Lamb, M. N. Yousaf, *Anal. Chem.* **2009**, *81*, 3297.
[37] R. H. Terrill, K. M. Balss, Y. Zhang, P. W. Bohn, *J. Am. Chem. Soc.* **2000**, *122*, 988.
[38] a) K. M. Balss, B. D. Coleman, C. H. Lansford, R. T. Haasch, P. W. Bohn, *J. Phys. Chem. B* **2001**, *105*, 8970; b) K. M. Balss, T.-C. Kuo, P. W. Bohn, *J. Phys. Chem. B* **2003**, *107*, 994.
[39] a) B. D. Coleman, N. Finnegan, P. W. Bohn, *J. Electroanal. Chem.* **2004**, *571*, 139; b) B. D. Coleman, N. Finnegan, P. W. Bohn, *Thin Solid Films* **2004**, *467*, 121.
[40] S. T. Plummer, P. W. Bohn, *Langmuir* **2002**, *18*, 4142.
[41] a) S. T. Plummer, Q. Wang, P. W. Bohn, R. Stockton, M. A. Schwartz, *Langmuir* **2003**, *19*, 7528; b) L. Liu, B. D. Ratner, E. H. Sage, S. Jiang, *Langmuir* **2007**, *23*, 11168.
[42] a) Q. Wang, P. W. Bohn, *J. Phys. Chem. B* **2003**, *107*, 12578; b) Q. Wang, J. A. Jakubowski, J. V. Sweedler, P. W. Bohn, *Anal. Chem.* **2004**, *76*, 1.
[43] Q. Wang, P. W. Bohn, *Thin Solid Films* **2006**, *513*, 338.
[44] a) X. Wang, P. W. Bohn, *J. Am. Chem. Soc.* **2004**, *126*, 6825; b) X. Wang, R. T. Haasch, P. W. Bohn, *Langmuir* **2005**, *21*, 8452.
[45] a) X. Wang, H. Tu, P. V. Braun, P. W. Bohn, *Langmuir* **2006**, *22*, 817; b) X. J. Wang, P. W. Bohn, *Adv. Mater.* **2007**, *19*, 515.
[46] S. Jayaraman, A. C. Hillier, *Langmuir* **2001**, *17*, 7857.
[47] E. L. May, A. C. Hillier, *Anal. Chem.* **2005**, *77*, 6487.
[48] E. L. Ratcliff, A. C. Hillier, *Langmuir* **2007**, *23*, 9905.
[49] T. Sehayek, A. Vaskevich, I. Rubinstein, *J. Am. Chem. Soc.* **2003**, *125*, 4718.
[50] T. Sehayek, T. Bendikov, A. Vaskevich, I. Rubinstein, *Adv. Funct. Mater.* **2006**, *16*, 693.
[51] T. Sehayek, D. Meisel, A. Vaskevich, I. Rubinstein, *Isr. J. Chem.* **2008**, *48*, 359.
[52] R. Yamada, H. Tada, *Langmuir* **2005**, *21*, 4254.
[53] S. E. Fosdick, J. A. Crooks, B.-Y. Chang, R. M. Crooks, *J. Am. Chem. Soc.* **2010**, *132*, 9226.
[54] a) S. E. Fosdick, K. N. Knust, K. Scida, R. M. Crooks, *Angew. Chem.* **2013**, *125*, 10632; *Angew. Chem. Int. Ed.* **2013**, *52*, 10438; b) G. Loget, D. Zigah, L. Bouffier, N. Sojic, A. Kuhn, *Acc. Chem. Res.* **2013**, *46*, 2513.
[55] C. Ulrich, O. Andersson, L. Nyholm, F. Björefors, *Angew. Chem.* **2008**, *120*, 3076; *Angew. Chem. Int. Ed.* **2008**, *47*, 3034.
[56] C. Ulrich, O. Andersson, L. Nyholm, F. Björefors, *Anal. Chem.* **2009**, *81*, 453.
[57] J. Isaksson, N. D. Robinson, M. Berggren, *Thin Solid Films* **2006**, *515*, 2003.
[58] S. Inagi, Y. Ishiguro, M. Atobe, T. Fuchigami, *Angew. Chem.* **2010**, *122*, 10334; *Angew. Chem. Int. Ed.* **2010**, *49*, 10136.
[59] Y. Ishiguro, S. Inagi, T. Fuchigami, *Langmuir* **2011**, *27*, 7158.
[60] N. Shida, Y. Ishiguro, M. Atobe, T. Fuchigami, S. Inagi, *ACS Macro Lett.* **2012**, *1*, 656.
[61] S. Inagi, H. Nagai, I. Tomita, T. Fuchigami, *Angew. Chem.* **2013**, *125*, 6748; *Angew. Chem. Int. Ed.* **2013**, *52*, 6616.
[62] a) S. Ramakrishnan, C. Shannon, *Langmuir* **2010**, *26*, 4602; b) R. Ramaswamy, C. Shannon, *Langmuir* **2011**, *27*, 878.
[63] a) T. R. Kline, W. F. Paxton, Y. Wang, D. Velegol, T. E. Mallouk, A. Sen, *J. Am. Chem. Soc.* **2005**, *127*, 17150; b) G. Loget, J. Roche, E. Gianessi, L. Bouffier, A. Kuhn, *J. Am. Chem. Soc.* **2012**, *134*, 20033.
[64] B. E. Collins, K. P. S. Dancil, G. Abbi, M. J. Sailor, *Adv. Funct. Mater.* **2002**, *12*, 187.
[65] L. M. Karlsson, P. Tengvall, I. Lundström, H. Arwin, *J. Electrochem. Soc.* **2002**, *149*, C648.
[66] K. Kant, S. P. Low, A. Marshal, J. G. Shapter, D. Losic, *ACS Appl. Mater. Interfaces* **2010**, *2*, 3447.
[67] C. M. Thompson, M. Nieuwoudt, A. M. Ruminski, M. J. Sailor, G. M. Miskelly, *Langmuir* **2010**, *26*, 7598.
[68] L. R. Clements, P.-Y. Wang, W.-B. Tsai, H. Thissen, N. H. Voelcker, *Lab Chip* **2012**, *12*, 1480.
[69] T. M. Day, P. R. Unwin, N. R. Wilson, J. V. Macpherson, *J. Am. Chem. Soc.* **2005**, *127*, 10639.
[70] T. S. Hansen, J. U. Lind, A. E. Daugaard, S. Hvilsted, T. L. Andresen, N. B. Larsen, *Langmuir* **2010**, *26*, 16171.
[71] W. S. Dillmore, M. N. Yousaf, M. Mrksich, *Langmuir* **2004**, *20*, 7223.
[72] E. W. L. Chan, M. N. Yousaf, *Mol. BioSyst.* **2008**, *4*, 746.
[73] J. Suzurikawa, M. Nakao, R. Kanzaki, H. Takahashi, *Sens. Actuators B* **2010**, *149*, 205.
[74] C. E. Carreón-González, J. De La Torre Medina, L. Piraux, A. Encinas, *Nano Lett.* **2011**, *11*, 2023.
[75] P. Kim, A. K. Epstein, M. Khan, L. D. Zarzar, D. J. Lipomi, G. M. Whitesides, J. Aizenberg, *Nano Lett.* **2012**, *12*, 527.
[76] P. Kim, W. E. Adorno-Martinez, M. Khan, J. Aizenberg, *Nat. Protoc.* **2012**, *7*, 311.
[77] R. Venkatasubramanian, K. Jin, N. S. Pesika, *Langmuir* **2011**, *27*, 3261.
[78] a) T. Z. Fahidy, *J. Appl. Electrochem.* **1983**, *13*, 553; b) R. A. Tacken, L. J. J. Janssen, *J. Appl. Electrochem.* **1995**, *25*, 1; c) J. M. D. Coey, G. Hinds, *J. Alloys Compd.* **2001**, *326*, 238.
[79] K. Tschulik, J. A. Koza, M. Uhlemann, A. Gebert, L. Schultz, *Electrochem. Commun.* **2009**, *11*, 2241.
[80] a) J. König, K. Tschulik, L. Büttner, M. Uhlemann, J. Czarske, *Anal. Chem.* **2013**, *85*, 3087; b) K. Tschulik, C. Cierpka, A. Gebert, L. Schultz, C. J. Kähler, M. Uhlemann, *Anal. Chem.* **2011**, *83*, 3275.
[81] a) P. Dunne, L. Mazza, J. M. D. Coey, *Phys. Rev. Lett.* **2011**, *107*, 024501; b) K. Tschulik, R. Sueptitz, M. Uhlemann, L. Schultz, A. Gebert, *Electrochim. Acta* **2011**, *56*, 5174.
[82] K. Tschulik, X. Yang, G. Mutschke, M. Uhlemann, K. Eckert, R. Sueptitz, L. Schultz, A. Gebert, *Electrochem. Commun.* **2011**, *13*, 946.
[83] K. Tschulik, C. Cierpka, G. Mutschke, A. Gebert, L. Schultz, M. Uhlemann, *Anal. Chem.* **2012**, *84*, 2328.
[84] M. Mrksich, *Acta Biomater.* **2009**, *5*, 832.
[85] Y. L. Khung, G. Barritt, N. H. Voelcker, *Exp. Cell Res.* **2008**, *314*, 789.
[86] A. M. D. Wan, R. M. Schur, C. K. Ober, C. Fischbach, D. Gourdon, G. G. Malliaras, *Adv. Mater.* **2012**, *24*, 2501.
[87] a) L.-Q. Wu, A. P. Gadre, H. Yi, M. J. Kastantin, G. W. Rubloff, W. E. Bentley, G. F. Payne, R. Ghodssi, *Langmuir* **2002**, *18*, 8620; b) J. Redepenning, G. Venkataraman, J. Chen, N. Stafford, *J. Biomed. Mater. Res. Part A* **2003**, *66A*, 411; c) X.-L. Luo, J.-J. Xu, Y. Du, H.-Y. Chen, *Anal. Biochem.* **2004**, *334*, 284; d) Y. Cheng, X. Luo, J. Betz, S. Buckhout-White, O. Bekdash, G. F. Payne, W. E. Bentley, G. W. Rubloff, *Soft Matter* **2010**, *6*, 3177.
[88] a) X.-W. Shi, C.-Y. Tsao, X. Yang, Y. Liu, P. Dykstra, G. W. Rubloff, R. Ghodssi, W. E. Bentley, G. F. Payne, *Adv. Funct.*

Mater. **2009**, *19*, 2074; b) X. Yang, E. Kim, Y. Liu, X.-W. Shi, G. W. Rubloff, R. Ghodssi, W. E. Bentley, Z. Pancer, G. F. Payne, *Adv. Funct. Mater.* **2010**, *20*, 1645.

[89] a) H. Yi, L.-Q. Wu, W. E. Bentley, R. Ghodssi, G. W. Rubloff, J. N. Culver, G. F. Payne, *Biomacromolecules* **2005**, *6*, 2881; b) G. F. Payne, E. Kim, Y. Cheng, H.-C. Wu, R. Ghodssi, G. W. Rubloff, S. R. Raghavan, J. N. Culver, W. E. Bentley, *Soft Matter* **2013**, *9*, 6019; c) W. Suginta, P. Khunkaewla, A. Schulte, *Chem. Rev.* **2013**, *113*, 5458.

[90] a) Y. Liu, E. Kim, R. V. Ulijn, W. E. Bentley, G. F. Payne, *Adv. Funct. Mater.* **2011**, *21*, 1575; b) Y. Liu, J. L. Terrell, C.-Y. Tsao, H.-C. Wu, V. Javvaji, E. Kim, Y. Cheng, Y. Wang, R. V. Ulijn, S. R. Raghavan, G. W. Rubloff, W. E. Bentley, G. F. Payne, *Adv. Funct. Mater.* **2012**, *22*, 3004.

[91] E. K. Johnson, D. J. Adams, P. J. Cameron, *J. Am. Chem. Soc.* **2010**, *132*, 5130.

[92] D. Wu, *Cell Res.* **2005**, *15*, 52.

[93] a) M. Mrksich, *Chem. Soc. Rev.* **2000**, *29*, 267; b) M. Mrksich, *MRS Bull.* **2005**, *30*, 180.

[94] a) J. Robertus, W. R. Browne, B. L. Feringa, *Chem. Soc. Rev.* **2010**, *39*, 354; b) I. Choi, W.-S. Yeo, *ChemPhysChem* **2013**, *14*, 55.

[95] M. N. Yousaf, M. Mrksich, *J. Am. Chem. Soc.* **1999**, *121*, 4286.

[96] M. N. Yousaf, B. T. Houseman, M. Mrksich, *Angew. Chem.* **2001**, *113*, 1127; *Angew. Chem. Int. Ed.* **2001**, *40*, 1093.

[97] W.-S. Yeo, M. N. Yousaf, M. Mrksich, *J. Am. Chem. Soc.* **2003**, *125*, 14994.

[98] M. N. Yousaf, B. T. Houseman, M. Mrksich, *Proc. Natl. Acad. Sci. USA* **2001**, *98*, 5992.

[99] a) E. W. L. Chan, M. N. Yousaf, *J. Am. Chem. Soc.* **2006**, *128*, 15542; b) E. W. L. Chan, M. N. Yousaf, *ChemPhysChem* **2007**, *8*, 1469.

[100] E. W. L. Chan, S. Park, M. N. Yousaf, *Angew. Chem.* **2008**, *120*, 6363; *Angew. Chem. Int. Ed.* **2008**, *47*, 6267.

[101] W. Luo, M. N. Yousaf, *J. Am. Chem. Soc.* **2011**, *133*, 10780.

[102] S. Jayaraman, E. L. May, A. C. Hillier, *Langmuir* **2006**, *22*, 10322.

[103] W. Zhan, J. Alvarez, R. M. Crooks, *J. Am. Chem. Soc.* **2002**, *124*, 13265.

[104] K.-F. Chow, B.-Y. Chang, B. A. Zaccheo, F. Mavre, R. M. Crooks, *J. Am. Chem. Soc.* **2010**, *132*, 9228.

[105] S. E. Fosdick, R. M. Crooks, *J. Am. Chem. Soc.* **2012**, *134*, 863.

[106] S. E. Fosdick, S. P. Berglund, C. B. Mullins, R. M. Crooks, *Anal. Chem.* **2013**, *85*, 2493.

[107] Y.-C. Chen, R. J. Young, J. V. Macpherson, N. R. Wilson, *J. Phys. Chem. C* **2007**, *111*, 16167.

[108] H. A. Burgoyne, P. Kim, M. Kolle, A. K. Epstein, J. Aizenberg, *Small* **2012**, *8*, 3502.

[109] A. K. Epstein, A. I. Hochbaum, K. Philseok, J. Aizenberg, *Nanotechnology* **2011**, *22*, 494007.

[110] K. Eriksson, L. Johansson, E. Gothelid, L. Nyholm, S. Oscarsson, *J. Mater. Chem.* **2012**, *22*, 7681.

[111] G. Loget, J. Roche, A. Kuhn, *Adv. Mater.* **2012**, *24*, 5111.

[112] Y. Y. Li, P. Kim, M. J. Sailor, *Phys. Status Solidi A* **2005**, *202*, 1616.

[113] L. Bonnemay, S. Hostachy, C. Hoffmann, J. Gautier, Z. Gueroui, *Nano Lett.* **2013**, *13*, 5147.

[114] L. Yang, A. Gomez-Casado, J. F. Young, H. D. Nguyen, J. Cabanas-Danés, J. Huskens, L. Brunsveld, P. Jonkheijm, *J. Am. Chem. Soc.* **2012**, *134*, 19199.

[115] a) P. Neirynck, J. Brinkmann, Q. An, D. W. J. van der Schaft, L.-G. Milroy, P. Jonkheijm, L. Brunsveld, *Chem. Commun.* **2013**, *49*, 3679; b) Q. An, J. Brinkmann, J. Huskens, S. Krabbenborg, J. de Boer, P. Jonkheijm, *Angew. Chem.* **2012**, *124*, 12399; *Angew. Chem. Int. Ed.* **2012**, *51*, 12233.

[116] C. C. A. Ng, A. Magenau, S. H. Ngalim, S. Ciampi, M. Chockalingham, J. B. Harper, K. Gaus, J. J. Gooding, *Angew. Chem.* **2012**, *124*, 7826; *Angew. Chem. Int. Ed.* **2012**, *51*, 7706.

[117] R. Walder, A. Honciuc, D. K. Schwartz, *Langmuir* **2010**, *26*, 1501.